A new miniaturized CPW-UWB antenna for healthcare monitoring

YAQEEN S. MEZAAL*
Mobile Communication and Computing Engineering Department, University for Information Technology and Communications, Iraq

A microstrip antenna tailored to function in the Ultra-Wideband (UWB) frequency range of 3.4226 GHz to 11.805 GHz is developed, simulated, and fabricated in this article. An FR4 substrate with a slotted patch radiator based on feeding mechanism of Coplanar Waveguide (CPW) has been employed. According to the results of this investigation, the antenna successfully covers the whole ultra-wideband frequency range, with an operational bandwidth of 8.3824 GHz under an input reflection coefficient of -10 dB. Unlike conventional planar or microstrip patch antennas, this design displays radiation patterns that go in both directions. This small antenna is exemplar for use in healthcare stations and Wireless Body Area Networks (WBANs) due to its lightweight design, good emission characteristics, and wide frequency range. Consequently, it offers a potential technical answer to the problem of how to improve healthcare initiatives' wireless communication and sensing capacities in the future. The power and energy results are based on safety standards, such as FCC and IEC regulations regarding electromagnetic exposure. By facilitating seamless data transmission, this antenna can play a crucial role in improving healthcare initiatives, particularly in the context of remote patient monitoring and telemedicine.

(Received October 13, 2024; accepted June 3, 2025)

Keywords: UWB, CPW, Slotted patch, Smallness, Telemedicine, Healthcare monitoring, FCC and IEC regulations

1. Introduction

Methods for making diagnosis and developing treatment plans have been utterly transformed by recent technological developments. Ultra wideband (UWB) has rapidly become a promising technology with the ability to improve medical imaging modalities due to its huge frequency range data transmission and reception capabilities [1, 2]. Medical imaging systems that use ultra wide band improve their efficiency, signal strength, and picture resolution. The development of compact microstrip UWB antennas is one area of emphasis for this technology integration [3]. Because of their compact size, low production cost, and ease of integration, these antennas are ideal for use with portable medical devices. This is especially helpful when aiming for a higher level of overall performance. Modern mobile healthcare places a premium on space and size, thus this downsizing is appropriate. Whether the application calls for precise imaging to diagnose a disease at an early stage or monitoring a procedure, this type of antenna is a good fit. Some have speculated that their ability to transmit and receive signals at very high frequencies would revolutionize medical imaging, leading to better health care and more accurate diagnoses [4, 5, 6]. Some of the design principles that define success in medical usage are a vulnerability to interference, the possibility of creating terminal impedance, radiation pattern stability, and the ability to generate or receive short pulse signals [7]. A tiny metamaterial UWB antenna with a high correlation factor was constructed by the authors of [8] for the purpose of identifying malignant cells in human tissue, such as breast cancer, heart failure, and stroke. In microwave imaging systems, this antenna functions as a picture sensor. If this antenna design can scan tumor simulants with a good correlation factor, it could be a useful image sensor.

One possible solution for biomedical wireless applications is the tiny, flat CPW-UWB antenna proposed in [1]. This antenna would use a fan-shaped slotted net patch radiator to function within an impedance bandwidth of 7.4 GHz. Typically, WBANs and healthcare stations make use of this antenna. Slots increase the operational frequency range and improve the impedance match. Additionally, a proposal for a microwave imaging system that uses ground penetrating radar (GPR) to detect breast cancer was put up [9]. This system would use an ultra-wideband microstrip antenna. Because of its suitable return loss, the suggested antenna successfully reconstructed images within the permitted bandwidth. In [10], it was shown how a microstrip patch antenna can be used for early detection of breast cancer. To test how well the antenna captured the signal, a three-dimensional breast model was employed, which included distributive permittivity and conductivity. Also explored at [11] was the possibility of using microwave imaging, and more especially ultra-wideband printed circular monopole antennas, PCMAs, to detect breast cancer. The proposed PCMA enhanced picture reconstruction and clutter suppression in breast cancer detection systems with its broadside radiation pattern and relatively large impedance bandwidth.

This study proposes a beneficial microstrip antenna design that operates in the UWB frequency range of 3.4226 GHz to 11.805 GHz. The suggested UWB

microstrip antenna has several potential uses in the medical field, such as in wearable health monitors, remote patient monitoring systems, and medical imaging technologies. As a result of its tiny size, wide bandwidth, and sound radiation properties, it is feasible to enhance communication and data transfer within healthcare facilities. Here is the outline of the manuscript: In Section 2, the design process for the proposed CPW-UWB antenna is detailed. This section also contains the antenna's scheme and its RLC equivalent circuit. Antenna bandwidth and radiation patterns are primarily shaped via the slotted radiating patch, which is discussed at length at the same section. The third part for the consideration provides an evaluation for the antenna's performance at greater depth. After that, we'll review the S11 response, which is connected to the reflection coefficient and impendence matching inside the UWB spectrum. A further way to look at patterns and gains is as metrics that measure the antenna's efficiency at transmitting signals and how it radiates energy at all directions. Section 4 showcases an in-depth details about fabricated prototype and S11 measurements as compared with simulated S11 response and RLC circuit response. In last section, the study concludes with a brief overview for the findings, touching on the advantages for the UWB microstrip antenna and its potential applications at healthcare. We also discuss possible avenues for future studies, such as tailoring the antenna to more sophisticated communication systems or making it more specifically designed for use with body-implanted medical devices.

2. Methodology

Systems that manage signals at high frequencies, such wireless communication systems, radar, and satellite communications, benefit greatly from the CPW design of UWB antenna. Many antenna designs at the UWB range have been published employing coplanar waveguides [12–17], due to their inherent broad bandwidth, small size, and easy integration with other circuits.

The particular antenna configuration and dimensions that will be discussed in this article are depicted in Fig. 1 and Table 1. Slotted patch antennas are more efficient because they make use of the various resonant frequencies generated by a compact area. Because it has such a large effect on the antenna's efficiency and frequency of operation, the substrate size (25 mm × 27 mm × 1.6 mm) must be taken into account in the design. We selected a dielectric constant of 4.4 and a loss tangent of 0.02.

In an effort to enhance the UWB features, it was also planned to conduct extensive research into a wide range of design decisions and dimensional parameters. Finally, by optimizing these parameters, the CST simulator achieved the best possible performance for signal transmission and reception spanning the UWB frequency range of 3.4226 GHz to 11.805 GHz. The antenna's compactness and bandwidth widening capabilities are enhanced by the slotted patch design, which allows for the inclusion of additional resonances for improved performance.

To reach an impedance match for signal transmission, a coaxial feed line is used to power the radiator, and a 50-ohm microstrip line is also employed. Antenna designers frequently choose this combination due to its ability to optimize power transfer while reducing reflection losses. Because the dielectric substrate, ground plane, and CPW feeder are all on the same plane, the layout also allows for a lower footprint. The overall antenna size and production costs are both decreased by this coplanar design.

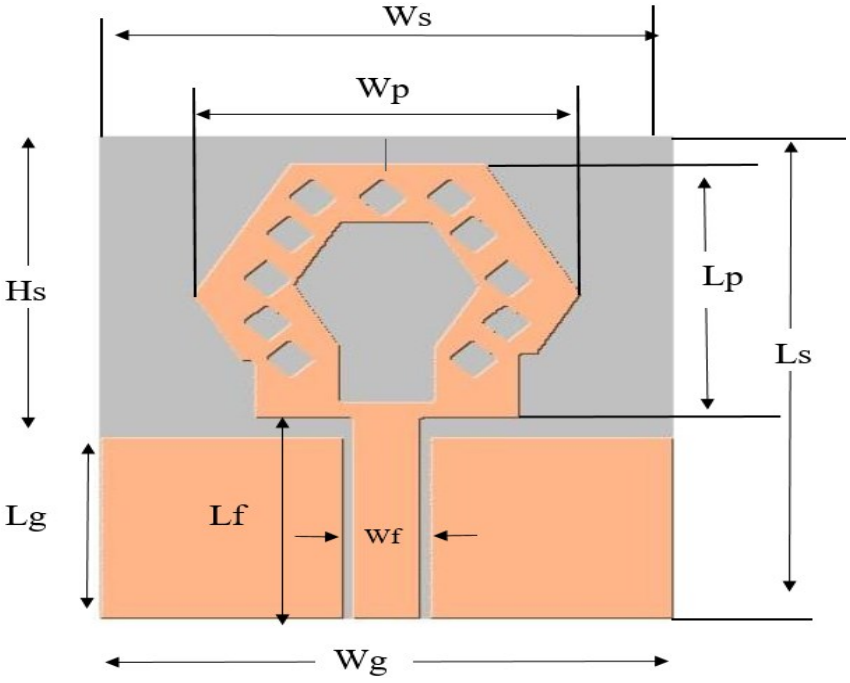

Fig. 1. Antenna topology and dimensions (colour online)

Table 1. Parameters design details for the modeled antenna

Parameter	Value (mm)
Ls	27
Ws	25
Hs	16.08
Lg	10.2
Wg	25
Lp	14.44
Wp	17
Lf	11.21
Wf	3.7

The RLC equivalent circuit, as projected by the microwave office simulator from the UWB antenna, is shown in Fig. 2. The connections between the capacitors and the resistors are parallel. By modifying the values of the capacitors and resistors in the circuit, one can alter the input reflection of an antenna. By switching up the inductor sequence, a wider variety of impedance bandwidths can be achieved. To achieve wide bands and multi-resonance properties, the top CPW-UWB antenna designs use RLC tank circuits. You can connect the three components of the RLC tank circuit, an inductor (L), a resistor (R), and a capacitor (C), in series or parallel to accommodate different frequencies. The improved performance of the antenna is a result of its increased frequency range. Radiation efficiency, the realized bandwidth (often called the Q factor), and tank size are three important factors that designers of CPW-UWB antennas should take into account when selecting an RLC tank circuit design. A matching impedance is required. By applying a definite value selection to components at the RLC tank circuit that control antenna resonances at different UWB spectrum regions, data transmission and reception can be maximized. Optimization and tuning of CPW-UWB antennas for more comprehensive band functioning using RLC tank circuits is not an easy task. It is common practice to utilize L1 to adjust the lower frequency band and L3 to adjust the upper frequency band in an RLC circuit, as shown in Fig. 2. You can adjust the input reflection and resonances by using other values of R and C elements.

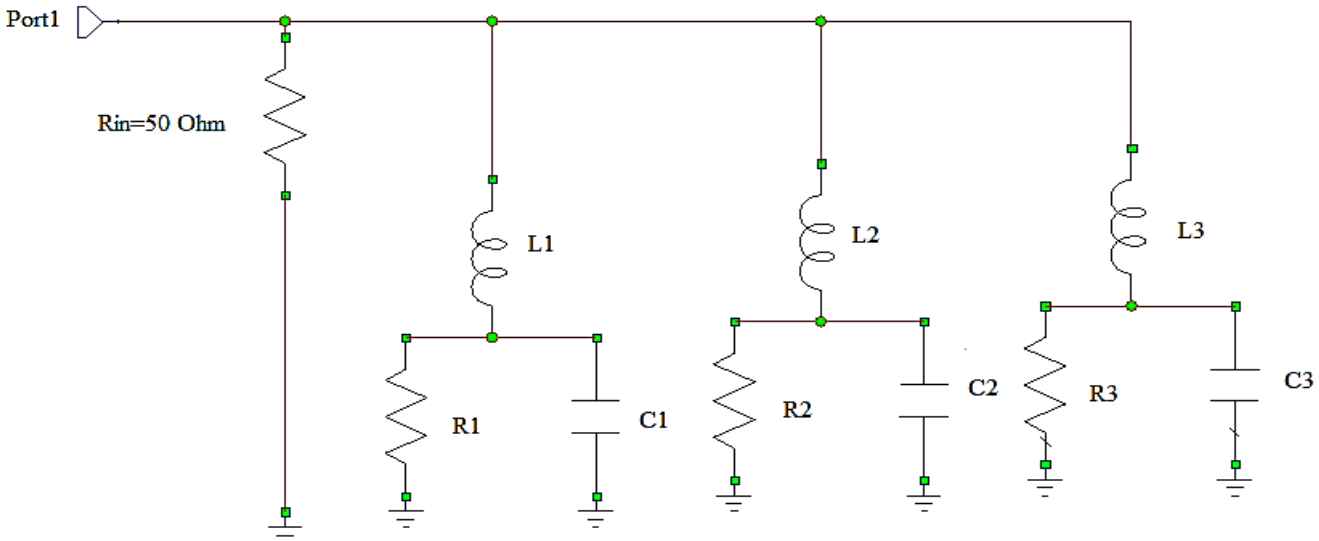

Fig. 2. The equivalent RLC circuit for the proposed CPW-UWB antenna. L1=5 nH, L2=30 nH, L3=1.1 nH, R1=1000 Ω, R2=4000 Ω, R3=3000 Ω, C1=1.1 pF, C2=0.01 pF, C3=0.1 pF

3. Simulation results

To gain a better understanding of the complicated aspects connected with suggested antennas, CST electromagnetic simulation tool is utilized to simulate the microstrip ultra-wideband coplanar waveguide (UWB-CPW) antenna with a wide operational bandwidth. The 3D and multilayered structural modeling capabilities of CST Microwave Studio make it a popular among antenna designers. Various circuit performance metrics, such as return loss, signal-to-noise ratio (SWR) as seen on a Smith chart, real power vs frequency, and electromagnetic field distributions at specific frequencies (E-field, H-field, etc.), can often be displayed and solved for by the program. In addition, we may test radiation patterns and gains, which are essential for understanding the antenna's performance once installed.

Fig. 3 displays the simulation results, which demonstrate a wideband frequency response spanning from 3.4226 GHz to 11.805 GHz, with a bandwidth of around 8.3824 GHz. for ultra-wideband (UWB) uses, the antenna's multi-frequency communication capabilities are paramount.

In addition, the modeling findings show that there is a central frequency of 7.6138 GHz and a very good impedance bandwidth of 8.3824 GHz. S11 parameter stands for return loss or input reflection: This measurement is extremely important for assessing the

operation of an antenna because it shows the amounts of power that are reflected into our radio system as a result of any impedance mismatch between the feed line and the antenna. Its power transfer efficiency and overall balance will be better with a lower return loss value. The outcome was a return loss of -29 dB, which is very good for UWB antennas and indicates that they reflect minimal incoming power; this is, in theory, acceptable for purpose of efficient design.

To show the overall nature of return loss at higher operational frequencies, Fig 3 depicts the projected antenna's S11 response. The antenna's capacity to retain suitable qualities throughout its design band and its suitability for UWB systems are demonstrated by this. In addition to proving the validity of the engineering decisions made during its design, the simulation findings demonstrate that the CPW- UWB antenna was a practical part of future communication and wireless systems.

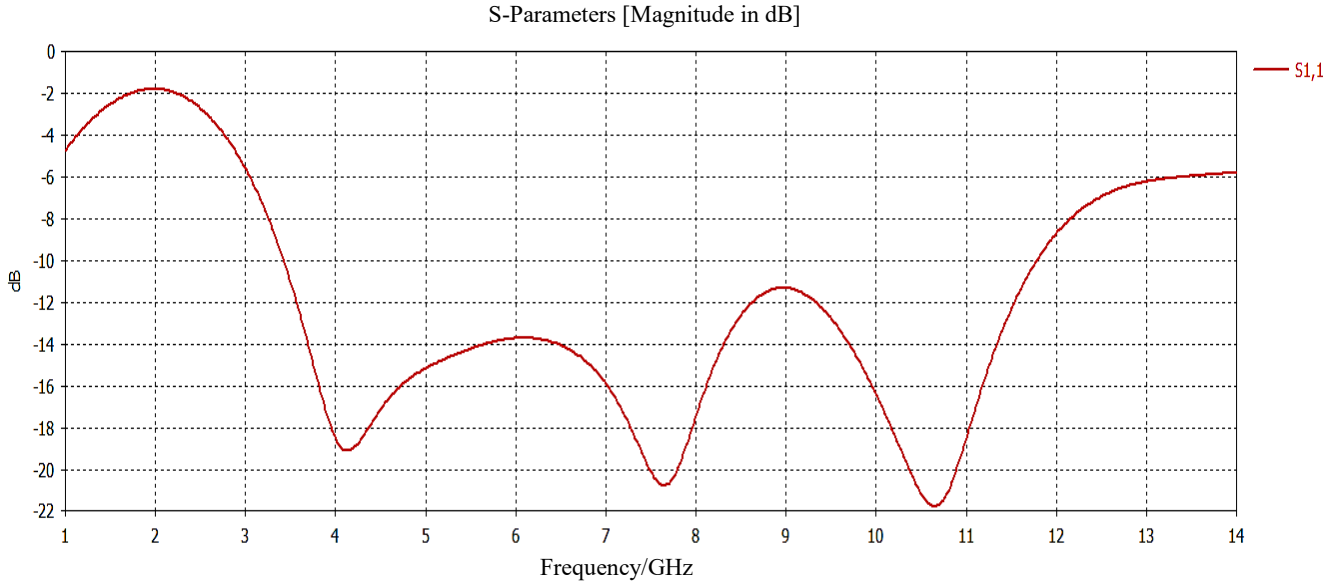

Fig. 3. Input reflection (S11) response for proposed UWB antenna

Fig. 4 depicts the 5.8 GHz UWB-CPW antenna's surface current distribution. It details the efficiency and performance at this frequency for a given matched or mismatched impedance and displays the current flow channels via the antenna structure. The feeding lines and the patch radiator have the widest surface current distribution, allowing them to absorb the most energy. Because of this concentration, the signal is efficiently conveyed through the feed line that connects to the patch. From what we can tell by looking at the patterns in the current distribution, the antenna is effectively radiating energy with little losses caused by improper loading. A high degree of power transmission was suggested by the highest magnetic field strength of 65.5 A/m, which was detected within the antenna structure. We found the strongest magnetic fields most frequently in the feeder region and at the patch radiator base. These areas are vital to the antenna's functioning since they greatly enhance radiation efficiency and directivity. Significantly elevated magnetic fields in these regions point to the utilization of electromagnetic principles in the design to modify radiation characteristics. The feeder is a direct feed device that feeds RF energy into the patch; thus, additional reflectors or directors are not required. Despite how tiny it seems, this apparently unimportant antenna component has a major influence on the efficiency and accuracy of the antenna's impedance matching. The patch keeps its style even with just two terminals. All the power you need to send (or receive, if necessary) can be supplied by connecting directly to the transmit or receive end. We can test the CPW- UWB antenna at several frequencies by measuring the surface current distribution and the strength of the magnetic field. The optimization of antenna designs for UWB applications necessitates these studies due to the remarkable efficiency and wide bandwidth requirements of these technologies.

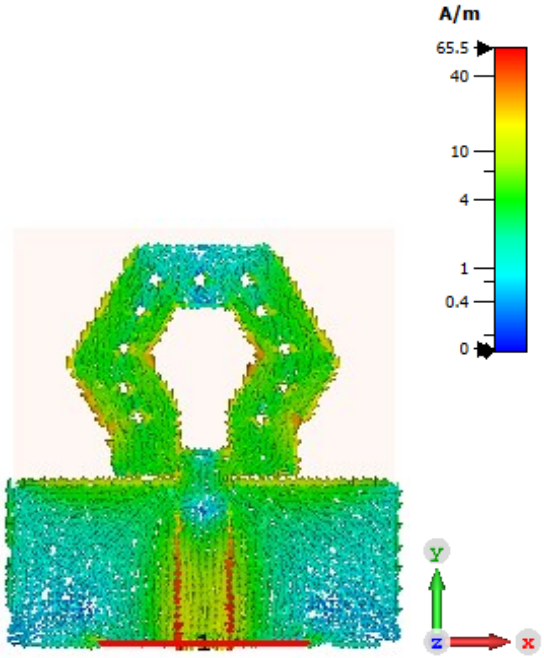

Fig. 4. Surface current intensity distribution for the CPW-UWB antenna (colour online)

At 7.2 GHz, the suggested UWB antenna depicted in Fig. 5, has three-dimensional radiation patterns. These patterns show the patterns of power radiated from the antenna into space, which can be used to estimate its directivity and global performance. At this operational frequency, the maximum gain of the proposed antenna is 3.07 dBi, which is partially explained by its moderate power. Our antenna's consistent performance in different directions is demonstrated by the 3D radiation patterns, which is useful for installations that demand error-free transmission in a variety of orientations. The antenna's 3.07 dBi gain proves that it improves its directionality in some space regions while keeping appropriate coverage in all others. This enhances signal coverage and integrity, especially for UWB applications. In addition, the radiation patterns' spatial distribution and shape can be used to estimate their polarization characteristics and potential interferences with surrounding equipment. After getting a feel for its limitations, this UWB antenna can blend in seamlessly with intricate communication networks.

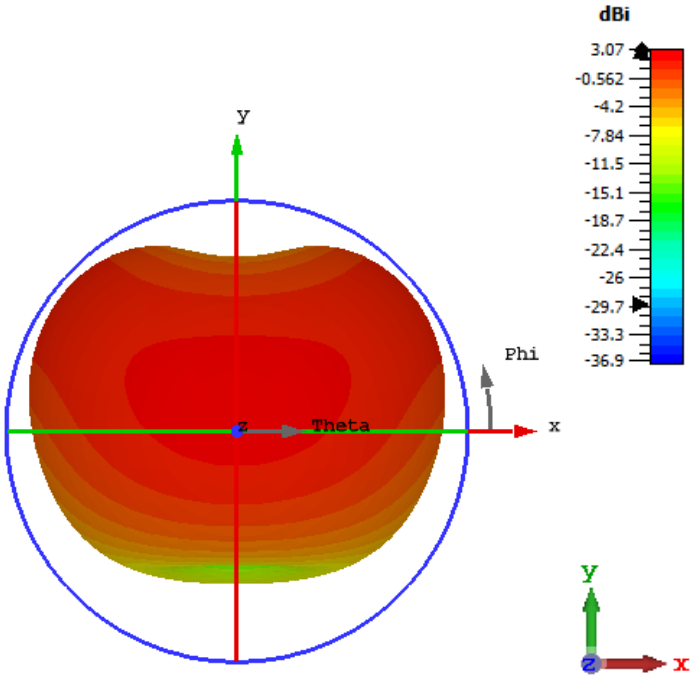

Fig. 5. 3D radiation patterns for the anticipated CPW-UWB antenna at 7.2 GHz (colour online)

Fig. 6 displays the UWB gain values for the proposed UWB antenna, which reach a peak of 11.2 dBi across the UWB frequency spectrum. You should already be aware that the antenna's gain is proportional to the square of the operating frequency. The main reasons for reduced efficiency in some frequency points include feedline-antenna impedance matching disruptions, dielectric loss, and conduction loss. The design of antennas relies heavily on losses, which can influence numerous aspects. An antenna's side lobes, caused by a drop in directivity, become noticeable when the antenna's size is larger than the wavelength. The antenna emits radiation in two different directions, as seen in Fig. 7. With its two huge radiation lobes on either side, this configuration demonstrates that the antenna is either receiving or radiating electromagnetic energy in two distinct directions. The bi-polar radiation pattern evenly disperses energy in two opposite directions and allows for symmetrical radiation around the antenna axis. Two significant peaks at the radiation pattern, each oriented at a different manner according to the antenna's construction, characterize this pattern, which is typical for bidirectional symmetrical radiation. The offset beam pattern of the bipolar radiation pattern allows signals to be sent in multiple directions, much as transpiration systems. The radiation pattern ensures consistent performance by displaying symmetrical behaviors across frequencies. To measure how well an antenna works, one compares the amount of power that goes into it from the generator to the amount that comes out of it. Magnetic, dielectric, and metal conduction losses are some of the causes of inefficient radiation and energy loss; ineffective radiation, however, radiates into space.

You can see the antenna design's total efficiency in Fig. 8. At 1.5 GHz, the efficiency is at its lowest point (-15.591 dB), and it grows substantially with frequency, reaching -0.51482 dB at 7 GHz.

In this section, we explore the performance metrics of the projected CPW-UWB antenna, focusing on substrate loss and power details, as shown in Fig. 9, along with the temporal field energy distribution depicted in Fig. 10. Substrate loss is a critical factor affecting antenna efficiency, representing the energy dissipated within the dielectric material. Our analysis includes quantitative measurements of substrate loss across the frequency range of 1.5 to 14 GHz and an examination of power output levels in relation to input power, highlighting the antenna's efficiency. We will compare these metrics against safety standards established by the Federal Communications Commission (FCC) and the International Electro technical Commission (IEC). Additionally, Fig. 10 illustrates the temporal distribution of field energy generated by the antenna, providing insights into how energy propagates over time and its implications for safe usage in healthcare environments. We will analyze the dynamic behavior of field energy and its correlation with patient safety, focusing on peak energy levels and their duration to assess potential risks associated with prolonged exposure. By ensuring that our findings align with established safety guidelines, we can confidently assert that our antenna design is both efficient and safe for medical applications, thereby reinforcing its practical applicability while prioritizing user safety in healthcare settings. Table 2 compares the proposed CPW-UWB antenna to current state-of-the-art antennas and shows how its tiny dimensions and extended impedance bandwidth stand out.

It can be candidate for health monitoring to transmit important biomedical information to the nearest medical stations in crisis and emergency situations. Also, it can be integrated with other RF and microwave devices or cloud systems in [25-34] as future trends.

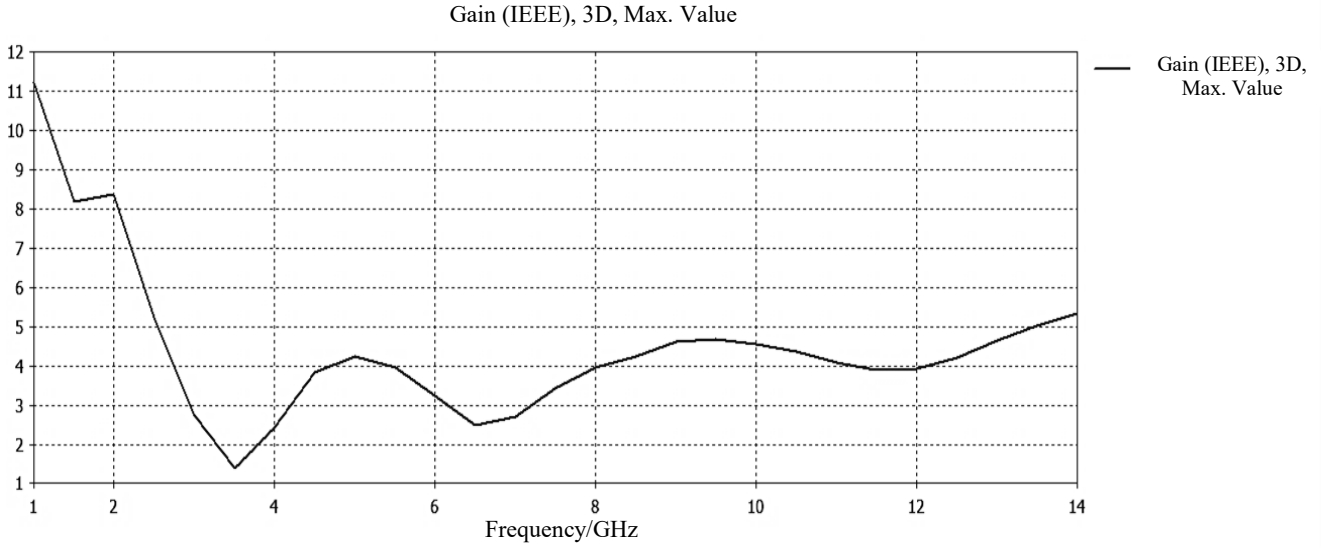

Fig. 6. Gain for designed CPW- UWB antenna (colour online)

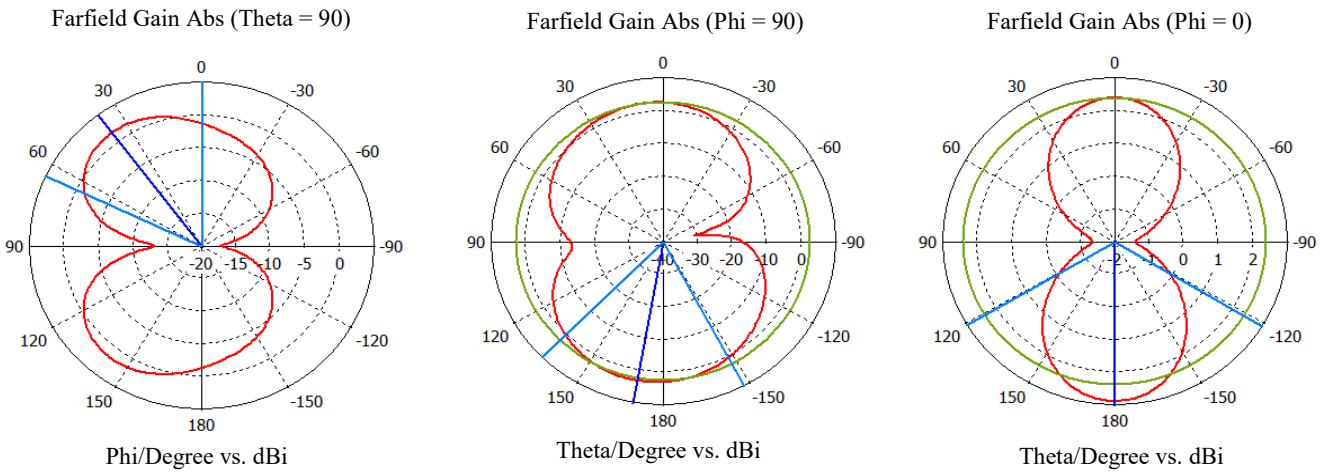

Fig. 7. Radiation patterns for projected CPW- UWB antenna at 7.2 GHz (colour online)

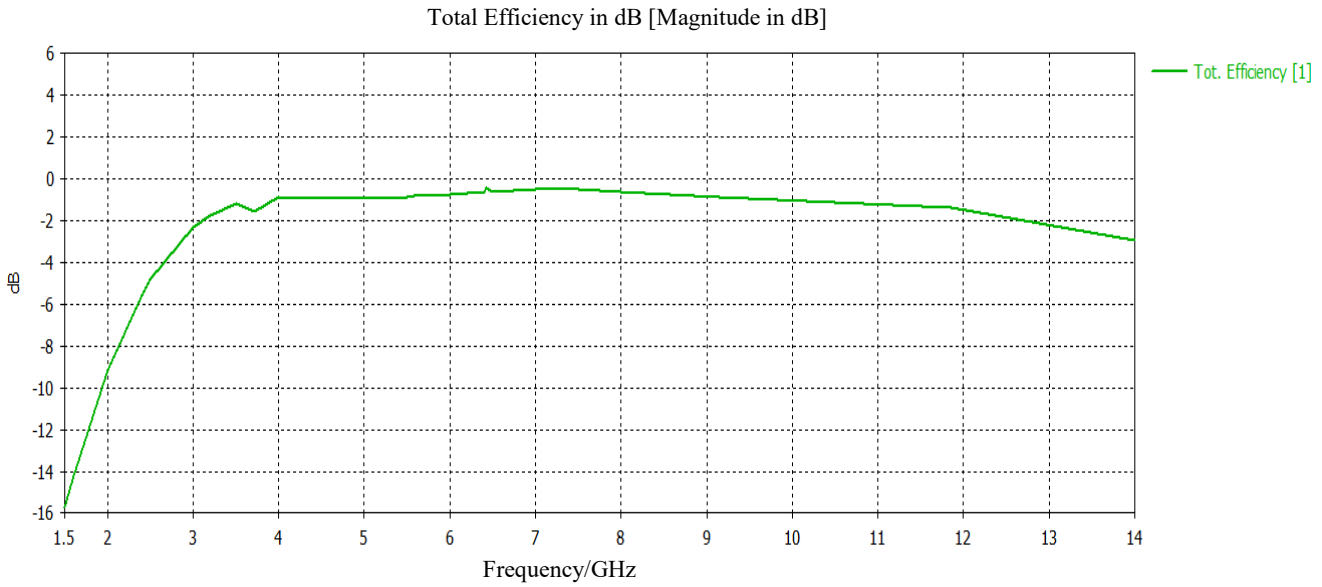

Fig. 8. Total radiation efficiency for the CPW- UWB antenna (colour online)

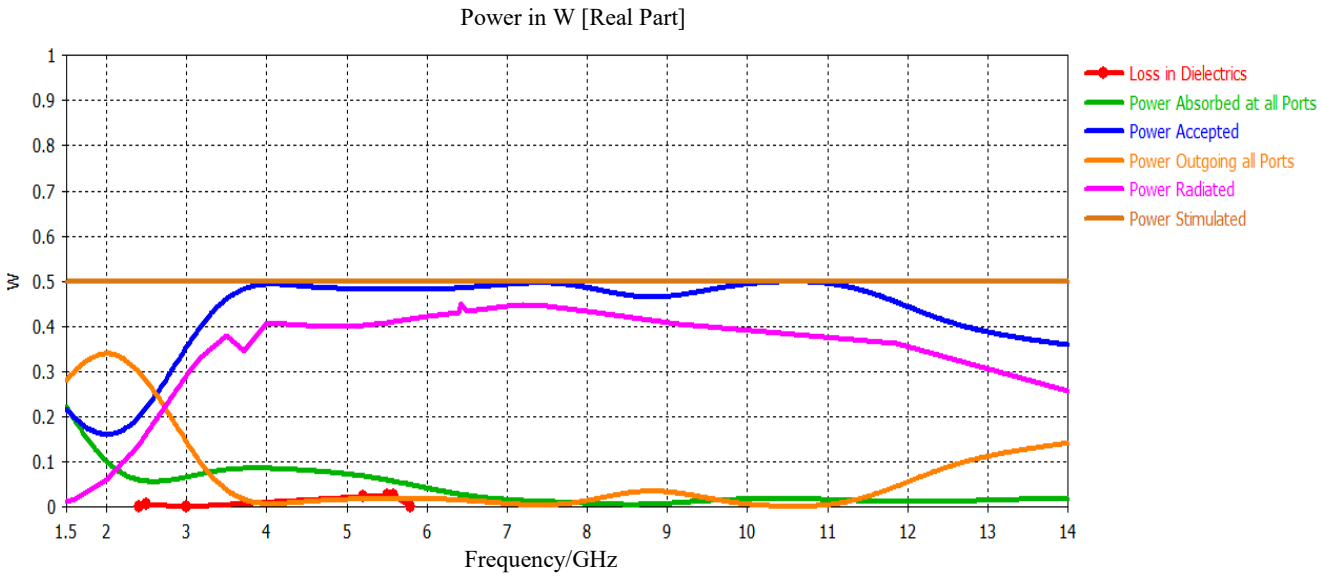

Fig. 9. All loss and power details for the projected CPW- UWB antenna (colour online)

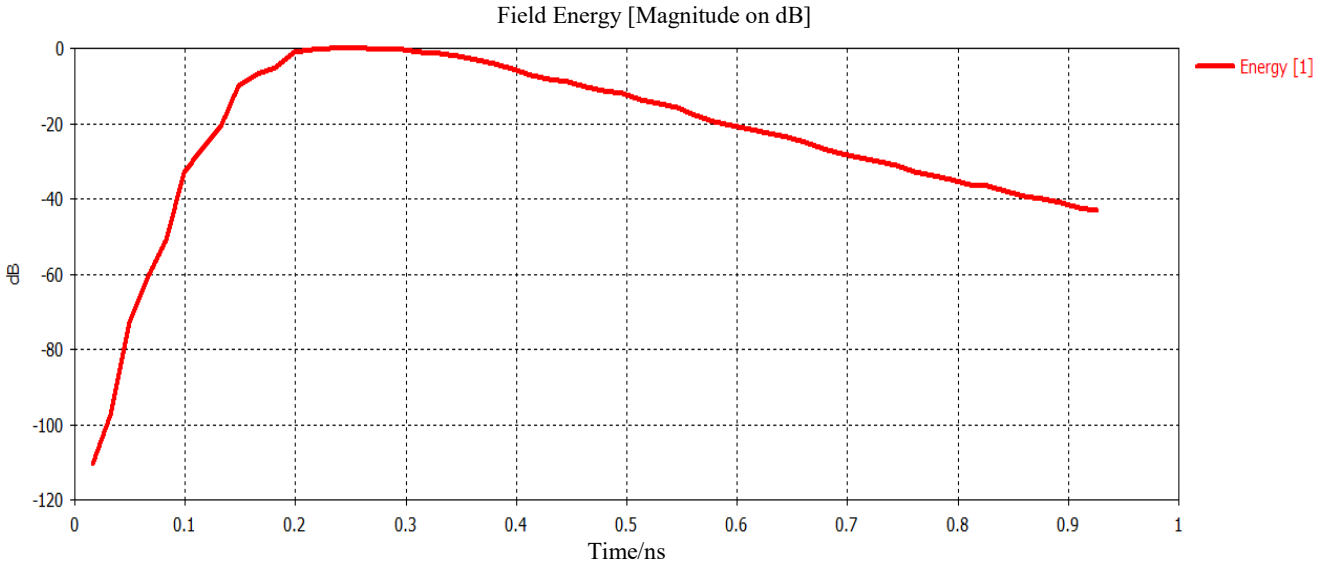

Fig. 10. Field energy over time for the projected CPW- UWB antenna (colour online)

Table 2. Comparison for our proposed antenna with other ones at the literature

Ref.	Dielectric Constant	Size (mm^2)	Bandwidth Range (GHz)	Applications
This work	4.4	25× 27	3.4226 -10.805	Healthcare Monitoring
[18]	3.16	40 × 38	2-12	Near-field microwave imaging
[19]	4.4	26 × 29	3.1–10.6	Near-field microwave imaging
[20]	10.2	19 × 19	2-8	Near-field microwave imaging
[21]	10.2	25 × 36	1-9	Near-field microwave imaging
[22]	10.2	50 × 50	1-9	Near-field microwave imaging
[23]	1.15–1.3	70.3 × 37	3-10	Microwave imaging systems
[24]	9	62.5 × 62.5	2–4.4	Microwave imaging systems

4. Fabrication and measurement

Fig. 11 displays a model of the microstrip CPW-UWB antenna built on a FR4 substrate with a thickness of 1.6 mm. We fine-tuned the proportions of the ground plane and patch according to the outcomes of the simulation. An S11 antenna and a VNA are linked through a coaxial wire.

The disparities between the input reflection responses of the built CPW-UWB antenna and the RLC equivalent circuit that was estimated are shown in Fig. 12. These manageable variances could have multiple causes. Manufacturing errors of a few microns are conceivable at antenna elements with accurate dimensions, no matter how careful one is. Even seemingly little differences in measured and simulated S11 responses can have a major impact on an antenna's efficiency. Antenna performance may be affected if dielectric qualities for FR-4 substrates are affected by manufacturing procedures that differ from the calculated material values. Inconsistent results at the loss tangent and dielectric could be one reason why the expected and observed S11 responses don't match up. Unaccounted for in the simulation are convection effects that might cause mysterious reflections during observations, which in turn affect S11 measurements. This explains why the experimental data and the simulation findings don't always match up. Reading errors could be caused by environmental factors that alter the S11 response, such as electromagnetic interference or surrounding objects. If these extraneous variables are left out of the simulations, we can see why the two data sets are different. It is possible to get inaccurate readings of the S11 response due to uncertainties caused by calibration errors at the vector network analyzer. There will be noticeable differences in the simulated reactions caused by even small calibration inaccuracies. When trying to replicate the design of a commercial microwave antenna, models could simplify or idealize details that aren't always accurate. These assumptions will lead to different results from simulations and measurements when dealing with complex or less-than-ideal behavior. Table 3 shows the results of comparing the projected antenna's input reflection responses to those of the measured, RLC equivalent circuit, and simulated versions. At -10 dB, the impedance bandwidths of the responses are slightly different as well as the center frequency for each case.

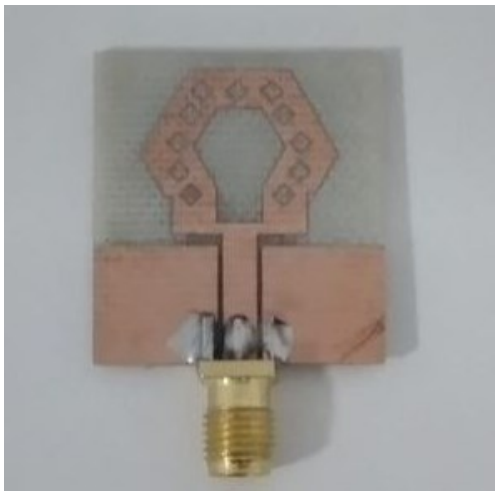

Fig. 11. A prototype for the projected antenna (colour online)

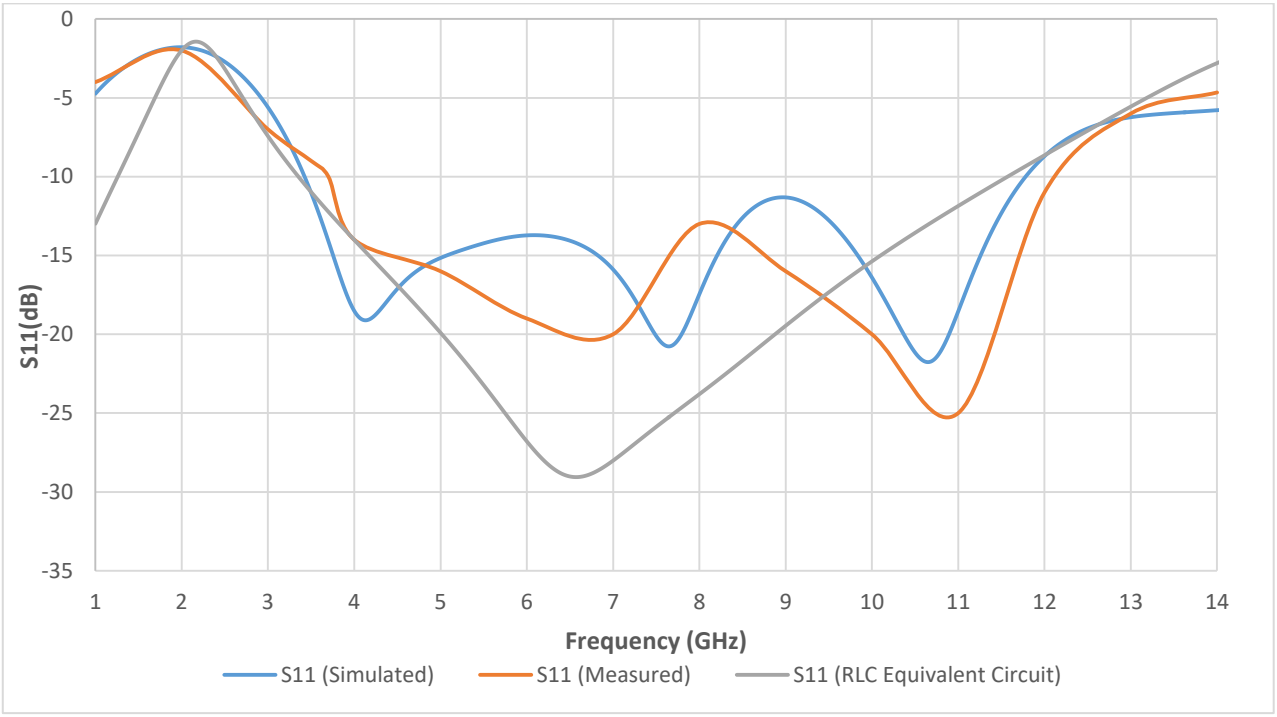

Fig. 12. Measured, RLC equivalent circuit and simulated input reflection responses for the projected antenna (colour online)

Table 3. Comparison for measured, RLC equivalent circuit and simulated input reflection responses for the projected antenna

Parameter	Measured Response	RLC Response	Simulated Response
BW magnitude	8.5	8.19	7.3824
Center Frequency (GHz)	7.95	7.455	7.1138
Relative BW Error as compared with the simulated parameter	15.1%	0.983%	…….
Relative center frequency error as compared with the simulated parameter	11.75 %	4.65 %	…….

5. Conclusion and future trends

Lastly, it is worth noting that the UWB microstrip antenna, constructed with a CPW feed line and a slotted patch on a FR-4 substrate, has demonstrated very good performance over a broad frequency range of 3.4226 GHz to 11.805 GHz, boasting a peak gain of 11.2 dBi. Among its many benefits, it is a good option for medical imaging and WBANs due to its small size, light weight, radiation patterns, and frequency responsiveness. One more thing that makes it promising is that it has bipolar radiation patterns. Another proof of this antenna's potential to facilitate groundbreaking healthcare advancements is its coverage of the whole UWB frequency band and its reliability in delivering communication in hospital settings. This antenna can boost wireless connectivity among medical devices by incorporating internationally recognized communication protocols.

Measurements of radiation patterns and gain can be part of future study to confirm the simulations' accuracy. The widespread implementation of cutting, edge antenna technologies in healthcare delivery has the potential to pave the way for future innovations and improved patient outcomes. Future developments in healthcare involving UWB microstrip antennas include their incorporation into IoT and wearable devices for real-time health monitoring, their seamless integration into medical applications made possible by advancements in miniaturization and flexibility, and the improvement of data transmission through the development of advanced communication protocols. Additionally, machine learning has the potential to enhance diagnostics by merging data transfer with vital sign detection. As the use of telehealth services increases, strong encryption solutions will be necessary to protect the confidentiality of patient information. Clinical trials testing UWB performance in real-world contexts and addressing regulatory compliance to ensure safety and efficacy should be part of future research to support global health initiatives in underserved countries.

References

[1] Y. S. Mezaal, Hind S. Ghazi, Ansam Qasim Kamil, Aqeel A. Al-Hillali, Kadhum Al-Majdi, Optoelectron. Adv. Mat. **18**(7-8), 353 (2024).

[2] B. Arif, M. Bilal, A. Quddus, R. Saleem, K. Ouahada, A. U. Rehman, M. F. Shafique, H. Hamam, IEEE Access **12**, 73247 (2024).

[3] M. B. Bicer, E. A. Aydin, Physical and Engineering Sciences at Medicine **44**(4), 1175 (2021).

[4] R. Singh, N. Narang, D. Singh, M. Gupta, Defence Science Journal **71**(3), 352 (2021).

[5] R. Samadianfard, J. Nourinia, C. Ghobadi, M. Shokri, Soft Computing **27**, 1 (2023).

[6] N. Iqbal, S. Karamzadeh, International Journal for Electronics, Mechanical and Mechatronics Engineering **7**(2), 1411 (2017).

[7] M. T. Islam, M. Samsuzzaman, I. Yahya, M. T. Islam, The Applied Computational Electromagnetics Society Journal (ACES) **33**, 1402 (2018).

[8] M. M. Islam, M. T. Islam, M. R. I. Faruque, M. Samsuzzaman, N. Misran, H. Arshad, Materials **8**(8), 4631 (2015).

[9] S. Adnan, R. A. Abd-Alhameed, H. I. Hraga, I. T. E. Elfergani, M. B. Child, 2010 Loughborough Antennas Propagation Conference, Loughborough, UK, pp. 389-392, 2010.

[10] R. Çalışkan, S. S. Gültekin, D. Uzer, Ö. Dündar, Procedia-Social and Behavioral Sciences **195**, 2905 (2015).

[11] I. M. Danjuma, M. O. Akinsolu, G. Oguntala, A. Asahraa, R. A. Abd-Alhameed, M. Bin-Melha, Loughborough Antennas & Propagation Conference, 2018.

[12] Adham R. Azeez, Sadiq K. Ahmed, Zaid A. Abdul Hassain, Amer Abbood Al-behadili, Hind S. Ghazi, Yaqeen S. Mezaal, Ahmed A. Hashim, Aqeel Ali Al-Hilali, Kadhum Al-Majdi, J. Mech. Contin. Math. Sci. **19**(3), 40 (2024).

[13] F. Abayaje, A. A. Alrawachy, Y. S. Mezaal, Optoelectron. Adv. Mat. **17**(7-8), 323 (2023).

[14] Y. S. Mezaal, Indian J. Sci. Technol. **9**(12), 1 (2016).

[15] Y. S. Mezaal, K. Al-Majdi, A. Al-Hilalli, A. A. Al-Azzawi, A. A. Almukhtar, Proceedings for the Estonian Academy of Sciences **71**(2), 194 (2022).

[16] D. O. Rodriguez-Duarte, J. A. T. Vasquez, R. Scapaticci, L. Crocco, F. Vipiana, IEEE Antennas Wireless Propag. Lett. **19**(12), 2057 (2020).

[17] M. Ojaroudi, S. Bila, M. Salimi, A Novel Approach for Brain Tumor Detection using Miniaturized High-Fidelity UWB Slot Antenna Array, European Conference on Antennas and Propagation, Mar 2019, Krakow, Poland. ffhal-02377024, 2019 [Online]. https://hal-unilim.archives-ouvertes.fr/hal-02377024.

[18] N. Tavassolian, S. Nikolaou, M. M. Tentzeris, Proceedings for the 2007 Asia-Pacific Microwave Conference, Bangkok, Thailand, Dec. 2007, pp. 1-4.

[19] T. S. See, Z. Chen, X. Qing, Proceedings for the 2009 Asia Pacific Microwave Conference, Singapore, Dec. 2009, pp. 2192-2195.

[20] Y. Wang, A. E. Fathy, M. R. Mahfouz, Proceedings of the 2011 IEEE International Symposium on Antennas and Propagation (APSURSI), Spokane, WA, USA, July 2011, pp. 2119-2122.

[21] X. Li, J. Yan, M. Jalilvand, T. Zwick, Proceedings of the 2012 6th European Conference on Antennas and Propagation (EUCAP), Prague, Czech Republic, March 2012, pp. 3677-3680.

[22] X. Li, Y. L. Sit, L. Zwirello, T. Zwick, Microw. Opt. Technol. Lett. **55**, 105 (2013).

[23] C. H. See, R. A. Abd-Alhameed, S. W. J. Chung, D. Zhou, H. Al-Ahmad, P. S. Excell, IEEE Trans. Antennas Propag. **60**, 2526 (2012).

[24] X. Yun, E. C. Fear, R. H. Johnston, IEEE Trans. Antennas Propag. **53**, 2374 (2005).

[25] Y. S. Mezaal, H. T. Eyyuboglu, J. K. Ali, 2013 13th

Mediterranean Microwave Symposium (MMS), **60**(3), 257 (2013).
[26] Y. S. Mezaal, H. T. Eyyuboğlu, J. K. Ali, IETE J. Res. **60**(3), 257 (2014).
[27] S. Roshani, S. Koziel, S. I. Yahya, M. A. Chaudhary, Y. Y. Ghadi, S. Roshani, L. Golunski, Sensors **23**(16), 7089 (2023).
[28] S. Roshani, S. I. Yahya, Y. S. Mezaal, M. A. Chaudhary, A. A. Al-Hilali, A. Mojirleilani, S. Roshani, Micromachines **14**(3), 553 (2023).
[29] S. K. Bavandpour, S. Roshani, A. Pirasteh, S. Roshani, H. Seyedi, AEU-International Journal of Electronics and Communications **135**, 153748 (2021).
[30] S. Roshani, K. Dehghani, S. Roshani, Frequenz **73**(7-8), 267 (2019).
[31] Y. S. Mezaal, H. T. Eyyuboglu, J. K. Ali, 2013 Third International Conference on Advanced Computing and Communication Technologies (ACCT), 2013.
[32] Y. S. Mezaal, A. S. Al-Zayed, Int. J. Electron. **106**(3), 477 (2019).
[33] Y. S. Mezaal, H. T. Eyyuboglu, PLoS One **11**(4), e0152615 (2016).
[34] Y. S. Mezaal, H. H. Madhi, T. Abd, S. K. Khaleel, Journal of Theoretical and Applied Information Technology **96**(20), 6937 (2018).

*Corresponding author: Yaqeen.mezaal@uoitc.edu.iq, yakeen_sbah@yahoo.com